Bioorganic & Medicinal Chemistry Letters 23 (2013) 1779–1785

Contents lists available at SciVerse ScienceDirect

Bioorganic & Medicinal Chemistry Letters

journal homepage: www.elsevier.com/locate/bmcl

Structure-based discovery of cellular-active allosteric inhibitors of FAK

Naoki Tomita [a,*], Yoko Hayashi [a], Shinkichi Suzuki [a], Yoshimasa Oomori [b], Yoshio Aramaki [a], Yoshihiro Matsushita [a], Misa Iwatani [a], Hidehisa Iwata [a], Atsutoshi Okabe [a], Yoshiko Awazu [a], Osamu Isono [a], Robert J. Skene [c], David J. Hosfield [c,†], Hiroshi Miki [a], Tomohiro Kawamoto [a], Akira Hori [a], Atsuo Baba [a]

[a] Pharmaceutical Research Division, Takeda Pharmaceutical Company Ltd, 26-1 Muraoka-Higashi 2-Chome, Fujisawa, Kanagawa 251-8555, Japan
[b] CMC Center, Takeda Pharmaceutical Company Ltd, 2-17-85 Jusohonmachi, Yodogawa-ku, Osaka 532-8686, Japan
[c] Takeda California, 10410 Science Center Drive, San Diego, CA 92121, United States

ARTICLE INFO

Article history:
Received 22 September 2012
Revised 8 January 2013
Accepted 15 January 2013
Available online 26 January 2013

Keywords:
FAK
Kinase
Inhibitors
Allosteric
Type III
Cancer
SBDD

ABSTRACT

In order to develop potent and selective focal adhesion kinase (FAK) inhibitors, synthetic studies on pyrazolo[4,3-*c*][2,1]benzothiazines targeted for the FAK allosteric site were carried out. Based on the X-ray structural analysis of the co-crystal of the lead compound, 8-(4-ethylphenyl)-5-methyl-1,5-dihydropyrazolo[4,3-*c*][2,1]benzothiazine 4,4-dioxide **1** with FAK, we designed and prepared 1,5-dimethyl-1,5-dihydropyrazolo[4,3-*c*][2,1]benzothiazin derivatives which selectively inhibited kinase activity of FAK without affecting seven other kinases. The optimized compound, *N*-(4-*tert*-butylbenzyl)-1,5-dimethyl-1,5-dihydropyrazolo[4,3-*c*][2,1]benzothiazin-8-amine 4,4-dioxide **30** possessed significant FAK kinase inhibitory activities both in cell-free (IC_{50} = 0.64 μM) and in cellular assays (IC_{50} = 7.1 μM). These results clearly demonstrated a potential of FAK allosteric inhibitors as antitumor agents.

Focal adhesion kinase (FAK) is a non-receptor tyrosine kinase and plays a key role in cell proliferation, resistance to apoptosis and anoikis, migration, and invasion.[1] Over expression of FAK is observed in a variety of tumors, and levels of FAK expression are correlated with grade of malignancy and poor prognosis.[1,2] Studies demonstrating suppression of FAK by using dominant-negative FAK or siRNA have shown both in vitro and in vivo tumor growth inhibitory activity.[3] A small molecule FAK inhibitor is potentially an effective anticancer agent for a broad range of tumors either administered alone or in combination with existing chemotherapies. Several inhibitors of FAK have been reported[4] and two of them were extensively examined in preclinical or clinical studies: PF-562271 from Pfizer is a dual inhibitor of FAK and Pyk2,[5] and NVP-TAE-226 from Novartis is a dual inhibitor of FAK and IGF1R (Fig. 1).[6] Both compounds were reported as Type I inhibitors (bound to ATP site) based on the X-ray co-crystal analyses.[5,6c] These inhibitors display remarkable inhibition of cancer cell growth in vitro and in vivo,[5–7] suggesting an FAK inhibitor with improved selectivity would be a desirable option for an anticancer therapy.

With the aim of developing novel FAK inhibitors that provide an inhibition profile differentiated from known FAK inhibitors, we

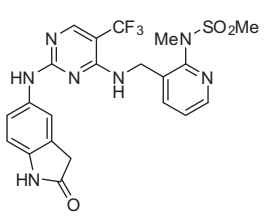

PF-562271
FAK/Pyk2 dual inhibitor

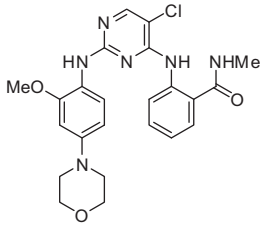

NVP-TAE-226
FAK/IGF1R dual inhibitor

Figure 1. ATP-competitive inhibitors of FAK.

* Corresponding author. Tel.: +81 466 32 1167; fax: +81 466 29 4448.
E-mail address: naoki.tomita@takeda.com (N. Tomita).
† Present address: Molecular Tagging Systems Inc., 1425 Russ Boulevard, San Diego, CA 92101, United States.

0960-894X/$ - see front matter © 2013 Elsevier Ltd. All rights reserved.
http://dx.doi.org/10.1016/j.bmcl.2013.01.047

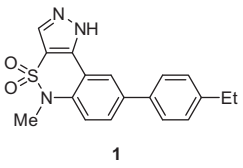

1

	FAK IC_{50} [μM]	
	pre-incubation	
ATP conc.	5 min	60 min
0.5 μM	1.2	0.96
1000 μM	6.4	2.9

Figure 2. HTS hit compound **1**.

carried out a systematic and exhaustive search to identify ATP-noncompetitive compounds.[8] High-throughput screening (HTS) of our internal compound library provided more than 10 hit compounds of different chemical classes. These hit compounds were evaluated using time-dependent assay (pre-incubation time: 5 min and 60 min) under high and low concentration of ATP (1000 and 0.5 μM). As a result, we found 1,5-dihydropyrazolo[4,3-*c*][2,1]benzothiazine **1**, which inhibited FAK kinase activity under the high concentration of ATP (Fig. 2).[9] The inhibitory activity at 1000 μM of ATP was slightly increased after 60-min preincubation.[10] Subsequent co-crystallization and X-ray structure determination of compound **1** in the FAK kinase domain revealed a novel binding mode in which compound **1** bound in a newly formed FAK allosteric site.[8,11] Since several Type III kinase inhibitors, such as allosteric inhibitors of MEK1/2[12] and Akt1/2,[13] possessed remarkable selectivity against other kinases,[14,15] we decided to develop FAK allosteric inhibitors starting from the lead compound **1**. We report herein our medicinal chemistry efforts on the discovery of novel allosteric FAK inhibitors by utilizing structure-based drug design.

X-ray crystallographic analysis of the co-crystal of compound **1** and FAK kinase domain revealed several polar and hydrophobic interactions (Fig. 3 PDB ID: 4EBV). The fused pyrazole ring interacts with the cationic side chain of Arg550 via cation–π interaction. One of the pyrazole nitrogens serves as a hydrogen bond donor to a water molecule. This water molecule seems to be displaceable by R^1, because its N^1-ethyl analogue **2** possessed similar inhibitory activity to **1**.[8] The *p*-ethylphenyl group might be transformed into another hydrophobic group to optimize hydrophobic interactions. Polar interaction with Gly563 or Asp564 also seems to be possible by introducing substituents as R^2.

Synthesis of pyrazolo[4,3-*c*][2,1]benzothiazine scaffold is described in Scheme 1. *N*-Methanesulfonylanthranilic acid esters **6**–**8** were prepared from commercially available methyl anthranilates **3** and **4**, and methyl 2-fluoro-4-nitrobenzoate **5** in 31–78% yield. Treatment of esters **6**–**8** with sodium hydride provided cyclized products **9**–**11** in 83–96% yield. Biphenyl derivative **12** was obtained from bromide **9** under typical Suzuki-coupling condition in 71% yield.[16] Subsequent treatment of the ketosultams **9**–**12** with *N*,*N*-dimethylformamide dimethylacetal followed by cyclocondensation with hydrazines afforded desired pyrazolo[4,3-*c*][2,1]benzothiazines **13**–**17** in a regioselective manner (80–96% yield). The regiochemistry of **17** was confirmed by X-ray crystallographic analysis.[17]

Terminal carboxamides **20**–**22** were prepared as described in Scheme 2. Bromide **13** was treated with 3,4-dihydro-2*H*-pyran (DHP) in the presence of TFA to give tetrahydropyran (THP)-protected pyrazolo[4,3-*c*][2,1]benzothiazine **18** (THP position was not determined) in 97% yield. Subsequent palladium-catalyzed coupling of **18** with 4-methoxycarbonylphenylboronic acid afforded a coupled product, which was converted to carboxylic acid **19** by saponification in 66% yield. Condensation of **19** with several amines followed by deprotection of THP group provided terminal carboxamides **20**–**22** in 40–55% yield.

Starting from intermediate 8-bromo-pyrazolo[4,3-*c*][2,1]benzothiazine **14**, nitrogen-linked pyrazolo[4,3-*c*][2,1]benzothiazines **23** and **24** were prepared by transition-metal mediated coupling reactions assisted with microwave irradiation (Scheme 3). Copper-mediated *C*–*N* coupling[18] of **14** with 4-fluorobenzamide provided carboxamide **23** in 46% yield, whereas palladium-catalyzed *C*–*N* coupling[19] with 4-fluoroaniline afforded phenylamine **24** in 22% yield.

The ester **15** was transformed into carbon-tethered analogues **25** and **26** (Scheme 4). Basic hydrolysis of **15** followed by condensation with 4-fluoroaniline provided amide **25** in 66% yield. Reduction of **15** with lithium aluminum hydride gave a corresponding carbinol, which was converted to amine **26** by mesylation and nucleophilic substitution in 13% yield.

8-Aminopyrazolo[4,3-*c*][2,1]benzothiazine derivatives **28**–**30** were prepared from corresponding 8-nitro intermediate **16** (Scheme 5). Compound **16** was reduced by hydrogenation to give aniline **27** in 96% yield. Reductive alkylation of **27** with 4-substituted benzaldehydes afforded benzylamines **28**–**30** in 35–77% yield.

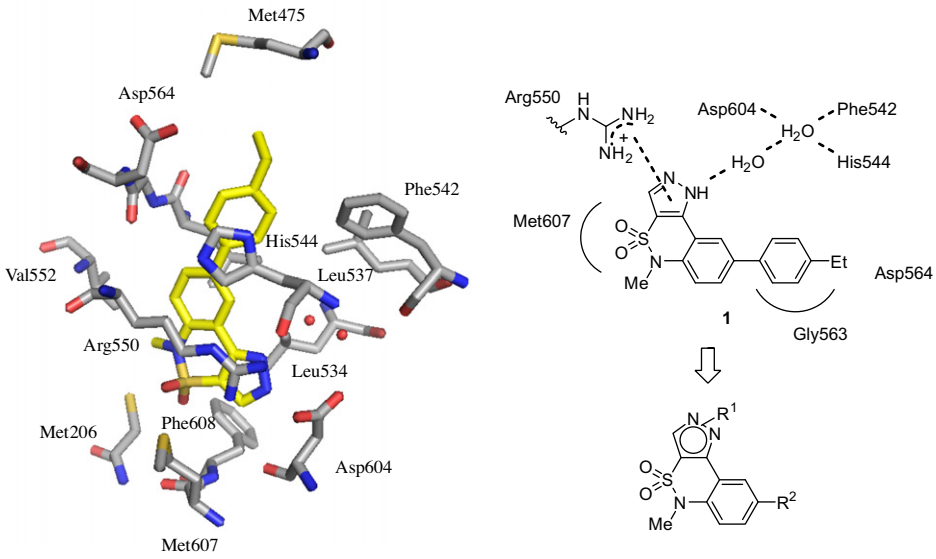

Figure 3. Structure-based design of pyrazolo[4,3-*c*][2,1]benzothiazines. PDB ID: 4EBV.

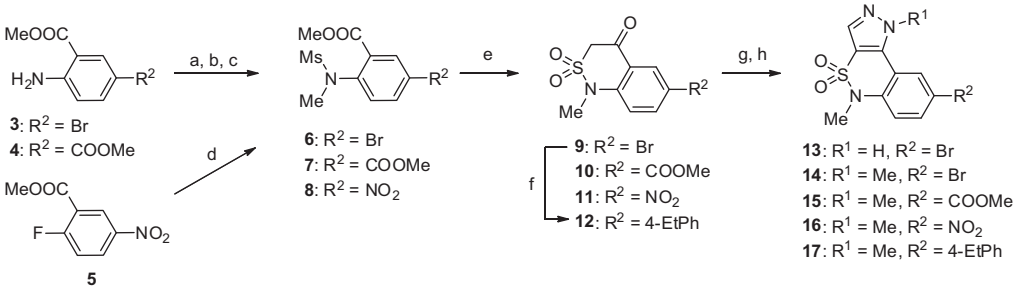

Scheme 1. Reagents and conditions: (a) MsCl, Et_3N, THF; (b) K_2CO_3, MeOH; (c) MeI, K_2CO_3, DMF; (d) MsNHMe, K_2CO_3, DMSO; (e) NaH, DMF or DMA; (f) 4-EtPhB$(OH)_2$, $Pd(OAc)_2$, PPh_3, Na_2CO_3, DME, H_2O, 150–170 °C, microwave; (g) DMFDMA, THF; (h) R^1NHNH_2, EtOH, reflux.

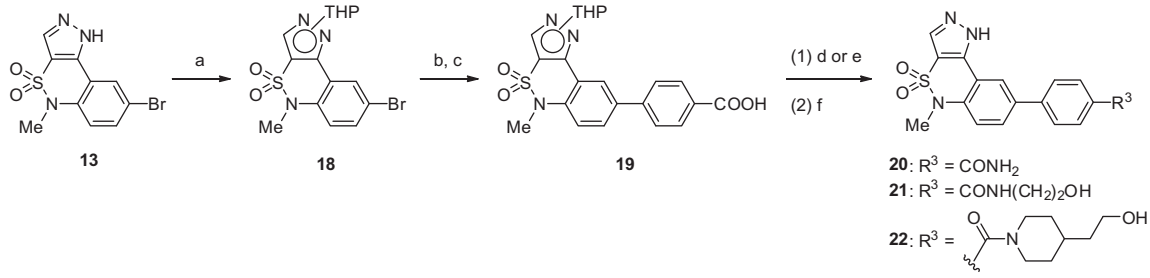

Scheme 2. Reagents and conditions: (a) DHP, TFA, THF, reflux; (b) 4-$MeO_2CPhB(OH)_2$, $PdCl_2(dppf)$, Et_3N, DME, H_2O, 150 °C, microwave; (c) NaOH, H_2O, MeOH, THF, DMA; (d) HOBt·NH_3, EDC, DMF; (e) amine, DMT-MM, THF, 2-propanol; (f) HCl, MeOH.

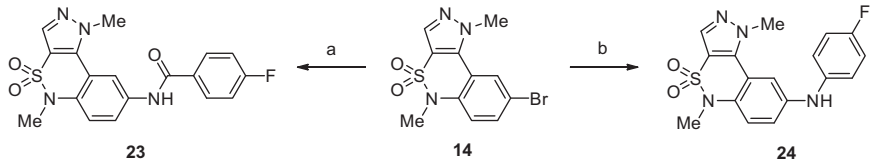

Scheme 3. Reagents and conditions: (a) 4-$FPhCONH_2$, CuI, *N,N′*-dimethylcyclohexane-1,2-diamine, K_2CO_3, DMA, 150–180 °C, microwave; (b) 4-$FPhNH_2$, $Pd_2(dba)_3$, X-phos, ^{t}BuONa, DMA, 150 °C, microwave.

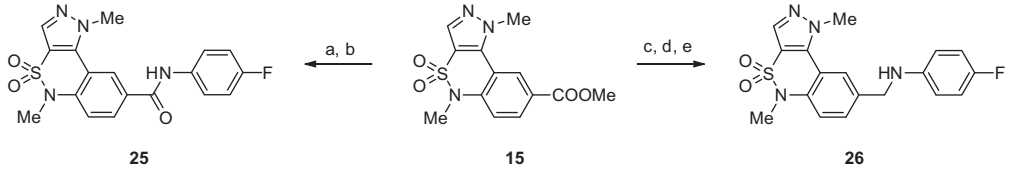

Scheme 4. Reagents and conditions: (a) NaOH aq, MeOH; (b) 4-$FPhNH_2$, EDC, HOBt, DMF; (c) $LiAlH_4$, THF; (d) MsCl, Et_3N, THF; (e) 4-$FPhNH_2$, Et_3N, THF.

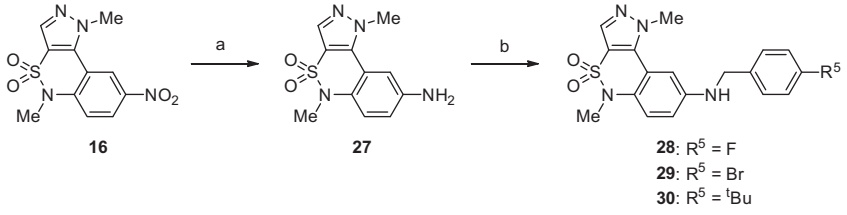

Scheme 5. Reagents and conditions: (a) Pd-C, H_2, MeOH, MeCN; (b) 4-R^5PhCHO, AcOH, MeCN, DMA, then $NaBH_4$.

Methylpyrazole regioisomer **31** was synthesized as described in Scheme 6. Suzuki coupling of bromide **18** with 4-ethylbenzeneboronic acid and subsequent deprotection of THP group gave pyrazolo[4,3-*c*][2,1]benzothiazine **1** in 60% yield. Alkylation of **1** with iodomethane gave a mixture of regioisomers **31** and **17**, both of which were isolated by column chromatography (81% and 14% isolated yield, respectively). Analytical data of the minor product was identical to the compound **17** prepared by a different method as described in Scheme 1.

FAK kinase inhibitory activities of pyrazolo[4,3-*c*][2,1]benzothiazines **20**–**22** bearing 4-substituted phenyl groups were evaluated as shown in Table 1. Since some compounds showed slow off-rate properties, enzymatic activity was measured after 60 min of pre-incubation to observe clearer response of time-dependent

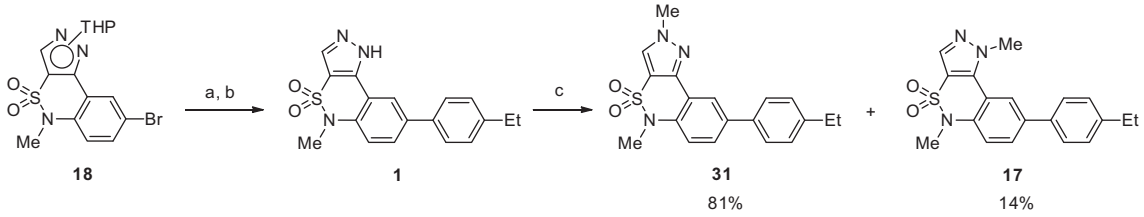

Scheme 6. Reagents and conditions: (a) 4-EtPhB(OH)$_2$, Pd(OAc)$_2$, PPh$_3$, Na$_2$CO$_3$, H$_2$O, DME, 150–170 °C, microwave; (b) HCl, MeOH; (c) MeI, K$_2$CO$_3$, DMF.

Table 1
SAR of substituents on the benzene ring

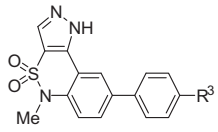

Compound	R^3	FAK IC$_{50}$[a] (μM)
1	Et	0.96
20	$CONH_2$	3.5
21	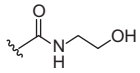	0.99
22	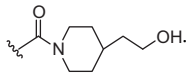	0.50

[a] ATP 0.5 μM, pre-incubation time 60 min.

inhibitors. Although lead compound **1** could also inhibit FAK in the presence of 1 mM of ATP, ATP concentration was fixed at 0.5 μM for higher sensitivity of the enzymatic assays.

4-Aminocarbonyl substitution resulted in a decrease of activity (**20**, IC$_{50}$ 3.5 μM) compared with that of 4-ethyl analogue (**1**, IC$_{50}$ 0.96 μM), but the activity was recovered by introduction of 2-hydroxyethyl group (**21**, IC$_{50}$ 0.99 μM). Since further elongation of the alcohol side chain increased inhibition activity (**22**, IC$_{50}$ 0.50 μM), it was suggested that some polar interactions might be acquired.

For the purpose of analyzing interactions between the carboxamide **22** and FAK, the crystal structure of **22** in the FAK kinase domain was accomplished (Fig. 4, PDB ID: 4I4E). The X-ray crystal structure revealed unambiguously that compound **22** did not induce formation of the FAK allosteric site, and was observed bound in the ATP binding site. The N-free pyrazole of **22** interacts with Glu500 and Cys502 in the hinge region by two hydrogen bonds. In addition, one of the oxygens of sulfonamide binds to the terminal amino group of Lys454. The terminal hydroxyl group of **22** forms direct and/or water-mediated hydrogen bonds with Glu506, Ser509, and Arg514. Considering the fact that the lead compound **1** could also bind to the allosteric site,[8] we supposed that N-free pyrazolo[4,3-*c*][2,1]benzothiazine analogues potentially possess two different binding modes: allosteric binding and hinge binding. This hypothesis was also supported by the fact that FAK inhibitory potential of compound **22** under the high concentration of ATP was much weaker (IC$_{50}$ >30 μM at ATP 1000 μM, preincubation time 60 min).

In order to facilitate pure allosteric inhibition of FAK, the potential hinge-binding motif of this chemotype should be modified. Guided by the crystallographic analysis and our previous studies,[8] we introduced a substituent on one pyrazole nitrogen to directly interfere with hydrogen bond formation at the hinge region. 1-Methyl and 2-methyl substituted pyrazolo[4,3-*c*][2,1]benzothiazines were evaluated as shown in Table 2. Introduction of methyl group on the 2-position of pyrazole resulted in drop of activity (**31**, IC$_{50}$ >30 μM). On the other hand, 1-methyl analogue **17** exhibited significant inhibition (IC$_{50}$ 0.077 μM), showing more than 10 times potent activity than those of **1** (IC$_{50}$ 0.96 μM) and **2** (IC$_{50}$ 2.1 μM).

In addition, compound **17** showed excellent kinase selectivity over a panel of seven kinases, including three kinases (Pyk2, Aurora B, and MEK1) which were weakly inhibited by N-free pyrazole **1** (Table 3). These results clearly demonstrated that introduction of the 1-methyl group on the pyrazolo[4,3-*c*][2,1]benzothiazine effectively altered the binding mode from dual to single (genuine allosteric), by disrupting hydrogen bond formation with hinge residues of kinases together with enhancing affinity to the allosteric site.

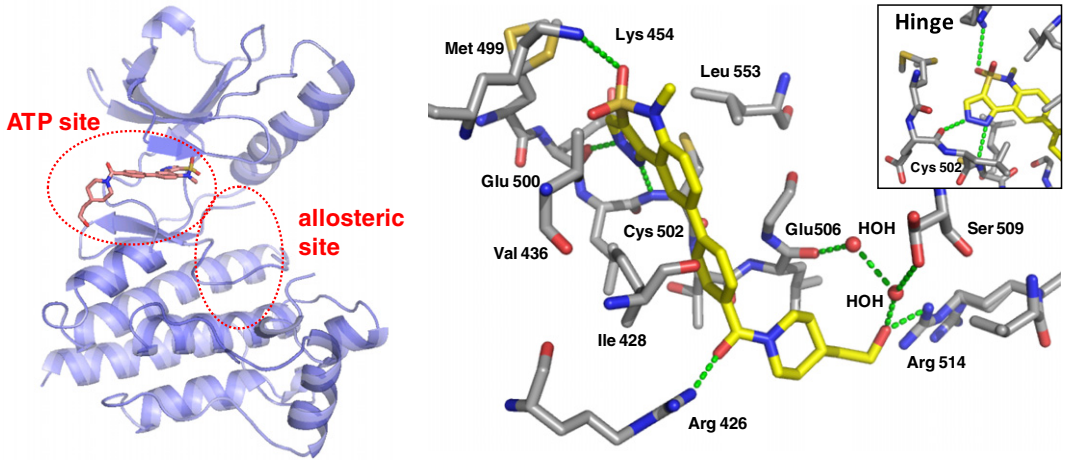

Figure 4. Co-crystal structure of **22** with FAK: hinge binding mode. PDB ID: 4I4E.

Table 2
SAR of substituents on the pyrazole ring

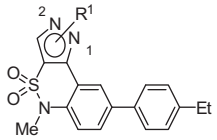

Compound	R^1	FAK IC_{50}[a] (μM)
1	H	0.96
17	1-Me	0.077
2	1-Et	2.1
31	2-Me	>30

[a] ATP 0.5 μM, pre-incubation time 60 min.

With the genuine FAK allosteric inhibitor in hand, we evaluated its inhibitory activity of intracellular FAK autophosphorylation (pFAK) by cell-based ELISA in PC3 M-luc cells.[20] Although compound **17** showed excellent enzymatic activity, its cellular activity was not sufficient (Table 4, pFAK 31% inhibition at 30 μM). We supposed that rigid biphenyl structure of **17** might limit its physicochemical properties and cellular potential. Thus, linker insertion between the 1-methylpyrazolo[4,3-*c*][2,1]benzothiazine core and the terminal phenyl group was examined (Table 4). Fortunately, three linkers were tolerated in the enzymatic assay, except for amide linker of **25** (FAK IC_{50} >30 μM). Among them, benzylamine **28** (FAK IC_{50} 0.32 μM, pFAK 85% inhibition at 30 μM) was selected as a new lead for further optimization because of its high potential of cellular activity.

Next, the aromatic side chain was optimized (Table 5). Although aniline **24** (FAK IC_{50} 4.3 μM, pFAK IC_{50} >30 μM) and *p*-bromo substitution on the benzyl unit **29** (FAK IC_{50} 1.4 μM, pFAK IC_{50} >30 μM) reduced activities, introduction of bulky *tert*-butyl group led to enhancement of cellular activity (**30**, FAK IC_{50} 0.64 μM, pFAK IC_{50} 7.1 μM). In addition, kinase selectivity profiles of **30** suggested that compound **30** was also a genuine allosteric inhibitor of FAK (Table 3). These results clearly demonstrated that inhibition of autophosphorylation of FAK with a small molecule by inducing FAK into an inactive conformation could be a novel strategy of modulating FAK signaling pathways. It is also noteworthy that this allosteric inhibition mode is highly specific to FAK. Unlike MEK1/2 and Akt1/2, FAK does not seem to share its allosteric site with the same subfamily kinase, Pyk2.[21]

Interaction of the optimized compound **30** with FAK kinase domain was examined in detail by X-ray crystallographic analysis (Fig. 5, PDB ID: 4I4F). The overall structure of the FAK kinase domain and binding site of **30** were similar to those observed in the complex of the lead compound **1**. The methyl substituent on the pyrazole ring is inserted in the hydrophilic space surrounded by Asp604 and His544, avoiding disruption of the hydrogen bond network of water molecules and presumably enhancing cation–π interaction between Arg550 and pyrazole ring by increasing electron density of the pyrazole. The 8-amino group gains a hydrogen bond with the backbone carbonyl of Gly563, while inducing a slight rotation of its side chain. The terminal *tert*-butyl group occupies a hydrophobic pocket formed by Met475, Leu486, Met499 (gatekeeper of FAK) and Val484. These interactions resulting from the induced structural rearrangement of the HRD-loop in FAK, facilitate the acquired slow-dissociative and ATP-noncompetitive-like properties observed with these compounds,[8] resulting in the intracellular inhibition of FAK autophosphorylation.

In summary, we have identified novel allosteric inhibitors of FAK, guided by the structural analyses of FAK-inhibitor complexes. Introduction of methyl group on the pyrazole ring effectively blocked potential hinge-binding mode and enhanced inhibition activity. Kinase inhibition profiles of 1-methyl derivatives showed excellent FAK selectivity over other kinases including Pyk2, which indicated this allosteric site was highly specific to FAK. A

Table 4
SAR of linker structure

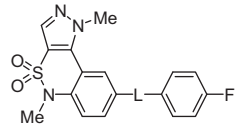

Compound	L	FAK IC_{50}[a] (μM)	Cell pFAK[b] (%inh.)
25	CONH	>30	Not tested
26	CH_2NH	2.0	4.8
23	NHCO	2.4	8.8
28	$NHCH_2$	0.32	85
17		0.077	31

[a] ATP 0.5 μM, pre-incubation time 60 min.
[b] At 30 μM.

Table 5
SAR of amino substituents

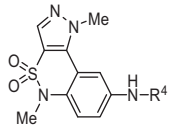

Compound	R^4	FAK IC_{50}[a] (μM)	Cell pFAK IC_{50} (μM)
24	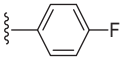	4.3	>30
28	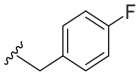	0.32	19
29	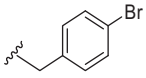	1.4	>30
30	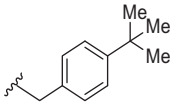	0.64	7.1

[a] ATP 0.5 μM, pre-incubation time 60 min.

Table 3
Kinase selectivity profiles of representative compounds

Compound	FAK IC_{50} (μM)	Tyrosine kinases IC_{50} (μM)			Serine threonine kinases IC_{50} (μM)			
		Pyk2	Src	HER2	Akt1	Aurora B	MEK1	p38α
1	1.2[a]/0.96[b]	9.0	>10	>10	>10	5.1	8.6	>10
17	0.42[a]/0.077[b]	>10	>10	>10	>10	>10	>10	>10
30	2.2[a]/0.64[b]	>10	>10	>10	>10	>10	>10	>10

[a] ATP 0.5 μM, pre-incubation time 5 min.
[b] ATP 0.5 μM, pre-incubation time 60 min.

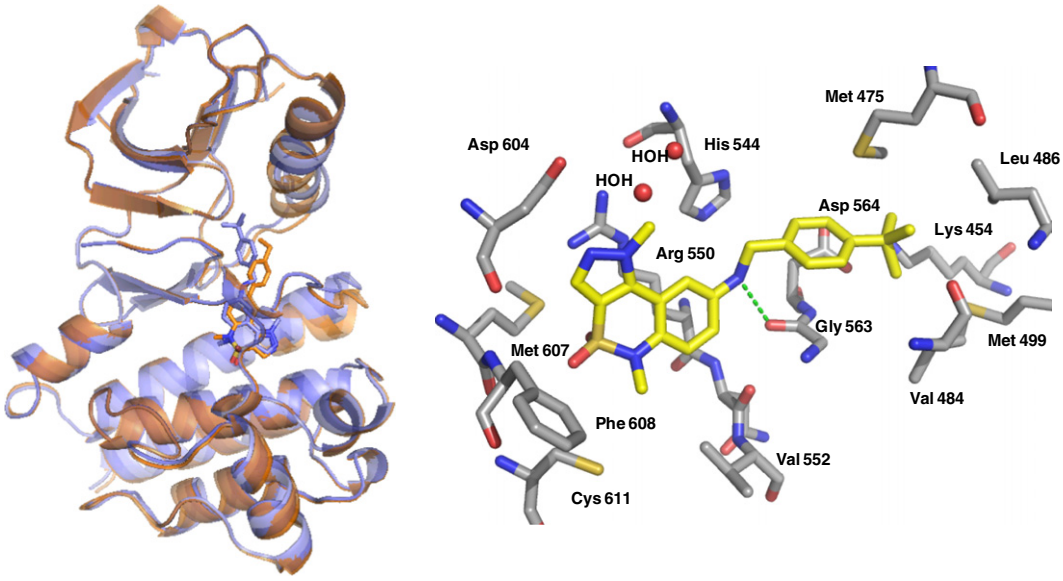

Orange: compound **1**
Purple: compound **30**

Figure 5. Co-crystal structure of **30** with FAK: allosteric binding mode. PDB ID: 4EBV (compound **1**), 4I4F (compound **30**).

benzylamine analogue **30** showed significant decrease of autophosphorylation of FAK in PC3M-luc cells, demonstrating that allosteric inhibitors could effectively block a key event of FAK signaling pathways in living cells. Further optimization of related compounds would provide allosteric inhibitors of FAK with enhanced activities and selectivity, which could be an option for novel molecular-targeted antitumor therapy.

Acknowledgments

We thank Clifford D. Mol and Gyorgy Snell for analyses of crystal structures and X-ray data collections. We thank Keiko Higashikawa and Mitsuyoshi Nishitani for analysis of X-ray single crystal analysis of compound **17**.

Supplementary data

Supplementary data (synthetic procedures of new compounds and X-ray single crystal analysis of compound **17**) associated with this article can be found, in the online version, at http://dx.doi.org/10.1016/j.bmcl.2013.01.047. These data include MOL files and InChiKeys of the most important compounds described in this article.

References and notes

1. (a) McLean, G. W.; Carragher, N. O.; Avizienyte, E.; Evans, J.; Brunton, V. G.; Frame, M. C. *Nat. Rev. Cancer* **2005**, *5*, 505; (b) Schlaepfer, D. D.; Hanks, S. K.; Hunter, T.; van der Geer, P. *Nature* **1994**, *372*, 786; (c) Ilic, D.; Furuta, Y.; Kanazawa, S.; Takeda, N.; Sobue, K.; Nakatsuji, N.; Nomura, S.; Fujimoto, J.; Okada, M.; Yamamoto, T.; Aizawa, S. *Nature* **1995**, *377*, 539; (d) Schwock, J.; Dhani, N.; Hedley, D. W. *Expert Opin. Ther. Targets* **2010**, *14*, 77.
2. Golubovskaya, V. M.; Kweh, F. A.; Cance, W. G. *Histol. Histopathol.* **2009**, *24*, 503. and references herein.
3. (a) Golubovskaya, V. M.; Zheng, M.; Zhang, L.; Li, J. L.; Cance, W. G. *BMC Cancer* **2009**, *9*, 280; (b) Schwock, J.; Dhani, N.; Cao, M. P. J.; Zheng, J.; Clarkson, R.; Radulovich, N.; Navab, R.; Horng, L. C.; Hedley, D. W. *Cancer Res.* **2009**, *69*, 4750; (c) Tsutsumi, K.; Yamaura, T.; Nakajima, M.; Honda, T.; Kawaoka, T. *Cancer Biol. Ther.* **2009**, *8*, 1292; (d) Halder, J.; Kamat, A. A.; Landen, C. N., Jr.; Han, L.; Lutgendorf, S. K.; Lin, Y. G.; Merritt, W. M.; Jennings, N. B.; Chaves-Reyes, A.; Coleman, R. L.; Gershenson, D. M.; Schmandt, R.; Cole, S. W.; Lopez-Berestein, G.; Sood, A. K. *Clin. Cancer Res.* **2006**, *12*, 4916.
4. (a) Slack-Davis, J. K.; Martin, K. H.; Tilghman, R. W.; Iwanicki, M.; Ung, E. J.; Autry, C.; Luzzio, M. J.; Cooper, B.; Kath, J. C.; Roberts, W. G.; Parsons, J. T. *J. Biol. Chem.* **2007**, *282*, 14845; (b) Walker, D. P.; Bi, F. C.; Kalgutkar, A. S.; Bauman, J. N.; Zhao, S. X.; Soglia, J. R.; Aspnes, G. E.; Kung, D. W.; Klug-McLeod, J.; Zawistoski, M. P.; McGlynn, M. A.; Oliver, R.; Dunn, M.; Li, J. C.; Richter, D. T.; Cooper, B. A.; Kath, J. C.; Hulford, C. A.; Autry, C. L.; Luzzio, M. J.; Ung, E. J.; Roberts, W. G.; Bonnette, P. C.; Buckbinder, L.; Mistry, A.; Griffor, M. C.; Han, S.; Guzman-Perez, A. *Bioorg. Med. Chem. Lett.* **2008**, *18*, 6071; (c) Walker, D. P.; Zawistoski, M. P.; McGlynn, M. A.; Li, J. C.; Kung, D. W.; Bonnette, P. C.; Baumann, A.; Buckbinder, L.; Houser, J. A.; Boer, J.; Mistry, A.; Han, S.; Xing, L.; Guzman-Perez, A. *Bioorg. Med. Chem. Lett.* **2009**, *19*, 3253; (d) Tanjoni, I.; Walsh, C.; Uryu, S.; Tomar, A.; Nam, J. O.; Mielgo, A.; Lim, S. T.; Liang, C.; Koenig, M.; Sun, C.; Patel, N.; Kwok, C.; McMahon, G.; Stupack, D. G.; Schlaepfer, D. D. *Cancer Biol. Ther.* **2010**, *9*, 764.
5. Roberts, W. G.; Ung, E.; Whalen, P.; Cooper, B.; Hulford, C.; Autry, C.; Richter, D.; Emerson, E.; Lin, J.; Kath, J.; Coleman, K.; Yao, L.; Martinez-Alsina, L.; Lorenzen, M.; Berliner, M.; Luzzio, M.; Patel, N.; Schmitt, E.; LaGreca, S.; Jani, J.; Wessel, M.; Marr, E.; Griffor, M.; Vajdos, F. *Cancer Res.* **1935**, *2008*, 68.
6. (a) Sakurama, K.; Noma, K.; Takaoka, M.; Tomono, Y.; Watanabe, N.; Hatakeyama, S.; Ohmori, O.; Hirota, S.; Motoki, T.; Shirakawa, Y.; Yamatsuji, T.; Haisa, M.; Matsuoka, J.; Tanaka, N.; Naomoto, Y. *Mol. Cancer Ther.* **2009**, *8*, 127; (b) Halder, J.; Lin, Y. G.; Merritt, W. M.; Spannuth, W. A.; Nick, A. M.; Honda, T.; Kamat, A. A.; Han, L. Y.; Kim, T. J.; Lu, C.; Tari, A. M.; Bornmann, W.; Fernandez, A.; Lopez-Berestein, G.; Sood, A. K. *Cancer Res.* **2007**, *67*, 10976; (c) Lietha, D.; Eck, M. J. *PLos ONE* **2008**, *3*, e3800.
7. (a) Bagi, C. M.; Roberts, G. W.; Andresen, C. J. *Cancer* **2008**, *112*, 2313; (b) Watanabe, N.; Takaoka, M.; Sakurama, K.; Tomono, Y.; Hatakeyama, S.; Ohmori, O.; Motoki, T.; Shirakawa, Y.; Yamatsuji, T.; Haisa, M.; Matsuoka, J.; Beer, D. G.; Nagatsuka, H.; Tanaka, N.; Naomoto, Y. *Clin. Cancer Res.* **2008**, *14*, 4631.
8. Iwatani, M.; Iwata, H.; Okabe, A.; Skene, R. J.; Mol, C. D.; Tomita, N.; Hayashi, Y.; Hosfield, D. J.; Hori, A.; Baba, A.; Miki, H. *Eur. J. Med. Chem.* 2012, In press.
9. For the measurement of enzymatic activity of FAK, we used HTRF detection system (Cisbio, France) with anti-phosphotyrosine antibody. Kinase buffer consisted of 50 mM Tris/HCl (pH 7.5), 5 mM $MgCl_2$, 5 mM $MnCl_2$, 2 mM DTT, 0.01% Tween20 and 0.01% BSA. 30 ng/mL of unphosphorylated FAK kinase domain and 5 μg/mL of poly-(GT)-biotin were optimal concentrations for the kinase reaction. After 5-min or 60-min of pre-incubation time of the enzyme and compounds, the kinase reaction was started with poly-(GT)-biotin and ATP (0.5 μM or 1000 μM). The kinase reaction was terminated by adding 60 mM EDTA diluted with detection buffer consisting of 50 mM HEPES (pH 7.0), 0.02% NaN_3, 0.1% BSA and 0.8 M KF. The detection mixture for phosphorylated poly-(GT)-biotin contained crypate-labeled PT66 and streptavidin-Xlent!. After incubation at room temperature for 1 h, the plates were read using EnVision 2102 Multilabel Reader (PerkinElmer). We set the total reaction without enzyme as 100% inhibitory activity and the total reaction as 0% inhibitory activity. Sigmoidal curves and IC_{50} values were estimated using 'Sigmoidal dose–response (variable slope)' with the top and bottom of the curve constrained at 100 and 0, respectively, in GraphPad Prism 5 Software (Ver 5.01). If the inhibitory activity was less than 50% under highest assayed concentration of compound, IC_{50} values would be not determined due to inaccuracy.

10. Since the difference of the two IC_{50} values (6.4 vs 2.9 μM) was not statistically significant, we performed dilution assay as reported previously.[8] Compound **1** showed slow dissociation kinetics with a half life of 19.4 min.
11. The co-crystal structure of compound **22** (Fig. 4) indicated compound **1** could also bind to the ATP site. The kinase selectivity, response to the phosphorylated kinase, and the docking model also suggested the potential hinge-binding mode of compound **1** as described previously.[8] We assumed compound **1** is a mixed-mode (allosteric and hinge-binding) inhibitor.
12. (a) Sebolt-Leopold, J. S.; Dudley, D. T.; Herrera, R.; van Becelaere, K.; Wiland, A.; Gowan, R. C.; Tecle, H.; Barrett, S. D.; Bridges, A.; Przybranowski, S.; Leopold, W. R.; Saltiel, A. R. *Nat. Med.* **1999**, *5*, 810; (b) Wallace, E. M.; Lyssikatos, J.; Blake, J. F.; Seo, J.; Yang, H. W.; Yeh, T. C.; Perrier, M.; Jarski, H.; Marsh, V.; Poch, G.; Livingston, M. G.; Otten, J.; Hingorani, G.; Woessner, R.; Lee, P.; Winkler, J.; Koch, K. *J. Med. Chem.* **2006**, *49*, 441; (c) Wallace, M. B.; Adams, M. E.; Kanouni, T.; Mol, C. D.; Dougan, D. R.; Feher, V. A.; O'Connell, S. M.; Shi, L.; Halkowycz, P.; Dong, Q. *Bioorg. Med. Chem. Lett.* **2010**, *20*, 4156.
13. (a) Lindsley, C. W.; Zhao, Z.; Leister, W. H.; Robinson, R. G.; Barnett, S. F.; Defeo-Jones, D.; Jones, R. E.; Hartman, G. D.; Huff, J. R.; Huber, H. E.; Duggan, M. E. *Bioorg. Med. Chem. Lett.* **2005**, *15*, 761; (b) Zhao, Z.; Leister, W. H.; Robinson, R. G.; Barnett, S. F.; Defeo-Jones, D.; Jones, R. E.; Hartman, G. D.; Huff, J. R.; Huber, H. E.; Duggan, M. E.; Lindsley, C. W. *Bioorg. Med. Chem. Lett.* **2005**, *15*, 905.
14. Recent reviews: (a) Klebl, B. M.; Müller, G. *Expert Opin. Ther. Targets* **2005**, *9*, 975; (b) Bogoyevitch, M. A.; Fairlie, D. P. *Drug Discovery Today* **2007**, *12*, 622; (c) Harrison, S.; Das, K.; Karim, F.; Maclean, D.; Mendel, D. *Expert Opin. Drug Discov.* **2008**, *3*, 761.
15. Recent examples of type III or type IV kinase inhibitors: (a) Converso, A.; Hartingh, T.; Garbaccio, R. M.; Tasber, E.; Rickert, K.; Fraley, M. E.; Yan, Y.; Kreatsoulas, C.; Stirdivant, S.; Drakas, B.; Walsh, E. S.; Hamilton, K.; Buser, C. A.; Mao, X.; Abrams, M. T.; Beck, S. C.; Tao, W.; Lobell, R.; Sepp-Lorenzino, L.; Zugay-Murphy, J.; Sardana, V.; Munshi, S. K.; Jezequel-Sur, S. M.; Zuck, P. D.; Hartman, G. D. *Bioorg. Med. Chem. Lett.* **2009**, *19*, 1240; (b) Xia, Z.; Knaak, C.; Ma, J.; Beharry, Z. M.; McInnes, C.; Wang, W.; Kraft, A. S.; Smith, C. D. *J. Med. Chem.* **2009**, *52*, 74; (c) Swann, S. L.; Merta, P. J.; Kifle, L.; Groebe, D.; Sarris, K.; Hajduk, P. J.; Sun, C. *Bioorg. Med. Chem. Lett.* **2010**, *20*, 5787; (d) Schneider, R.; Becker, C.; Simard, J. R.; Getlik, M.; Bohlke, N.; Janning, P.; Rauh, D. *J. Am. Chem. Soc.* **2012**, *134*, 9138.
16. Miyaura, N.; Suzuki, A. *Chem. Rev.* **1995**, *95*, 2457.
17. X-ray crystallographic data for compound **17** has been deposited with the Cambridge Crystallographic Data Center as CCDC 882940. Further information is described in the Supplementary data.
18. Klapars, A.; Antilla, J. C.; Huang, X.; Buchwald, S. L. *J. Am. Chem. Soc.* **2001**, *123*, 7727.
19. Huang, X.; Anderson, K. W.; Zim, D.; Jiang, L.; Klapars, A.; Buchwald, S. L. *J. Am. Chem. Soc.* **2003**, *125*, 6653.
20. Human prostate cancer PC3M-luc cells were purchased from Xenogen (Alameda, CA), and cultured in minimum essential medium supplemented with 10% fetal bovine serum in an incubator containing 5% CO_2. Cells (5×10^4 cells/100 μL) were seeded into low-attachment 96-well plate (Corning, Cat#3363) in culture medium with serially diluted compounds. After 30 min incubation, the cell suspension was transferred to the fibronectin-coated 96-well plate (BD, Cat#354402) and incubated for 2 h. After removing culture medium, cells were lysed in 50 μL of RIPA buffer (SIGMA, Cat#R0278). Lysates were transferred to the rabbit anti-FAK antibody immobilized plate (STAR phospho-FAK^{Tyr397} ELISA kit, Upstate, Cat#17-480), and incubated with anti-phospho FAK^{Tyr397} antibody for 2 h. After washing, a horseradish peroxidase (HRP)-labeled anti-rabbit IgG was added and plates were incubated for 30 min. After washing, HRP substrate was added and the plate was incubated for further 30 min. Then, the HRP reaction was measured in the absorbance at 450 nm.
21. Buckbinder, L.; Crawford, D. T.; Qi, H.; Ke, H. Z.; Olson, L. M.; Long, K. R.; Bonnette, P. C.; Baumann, A. P.; Hambor, J. E.; Grasser, W. A., III; Pan, L. C.; Owen, T. A.; Luzzio, M. J.; Hulford, C. A.; Gebhard, D. F.; Paralkar, V. M.; Simmons, H. A.; Kath, J. C.; Roberts, W. G.; Smock, S. L.; Guzman-Perez, A.; Brown, T. A.; Li, M. *Proc. Natl. Acad. Sci. U.S.A.* **2007**, *104*, 10619.